Crossover from antipersistent to persistent behavior in time series possessing the generalyzed dynamic scaling law

Alexander S. Balankin,[1,2] Oswaldo Morales Matamoros,[1] Ernesto Gálvez M.,[3] and Alfonso Pérez A.[2]
[1]*Sección de Posgrado e Investigación, ESIME, Instituto Politécnico Nacional, México D.F. 07738, Mexico*
[2]*Instituto Mexicano de Petróleo, México D.F. 07730, Mexico*
[3]*Departamento de Economía, Universidad de Sonora, Sonora 83000, Mexico*
(Received 8 October 2003; revised manuscript received 11 December 2003; published 31 March 2004)

The behavior of crude oil price volatility is analyzed within a conceptual framework of kinetic roughening of growing interfaces. We find that the persistent long-horizon volatilities satisfy the Family-Viscek dynamic scaling ansatz, whereas the mean-reverting in time short horizon volatilities obey the generalized scaling law with continuously varying scaling exponents. Furthermore we find that the crossover from antipersistent to persistent behavior is accompanied by a change in the type of volatility distribution. These phenomena are attributed to the complex avalanche dynamics of crude oil markets and so a similar behavior may be observed in a wide variety of physical systems governed by avalanche dynamics.

DOI: 10.1103/PhysRevE.69.036121 PACS number(s): 89.75.Da, 89.65.Gh, 05.40.−a, 05.45.Tp

I. INTRODUCTION AND BACKGROUND

Dynamics of all realistic complex systems always exhibits some part of randomness, either due to internal reasons, specific for nonlinear dynamical systems, or caused by external stochastic noise. Examples include many physical, biological, computer, social, and economic systems [1]. These systems commonly exhibit dynamic scaling invariance, i.e., their behavior does not change under rescaling of variables (for example, space and time) combined with an appropriate rescaling of the observables (Z) and the control (X,t) parameters [2,3]. In such a case, the randomness of spatiotemporal behavior may be characterized by the fluctuations of observable parameters, defined as $\sigma(\Delta,t)=\langle\langle[Z(X,t)-\langle Z(X,t)\rangle_\Delta]^2\rangle_\Delta\rangle_R^{1/2}$, where $\langle\cdots\rangle_\Delta$ denotes the spatial average within a window of size Δ and $\langle\cdots\rangle_R$ denotes the average over different realizations.

Typically, it is expected that the dynamic scaling invariance implies that fluctuations $\sigma(\Delta,t)$ satisfy the celebrated Family-Viscek dynamic scaling ansatz [4]

$$\sigma(\Delta,t)\propto t^{\beta} f(\Delta/\xi^{z}(t)) \tag{1}$$

where $\xi(t)\propto t^{1/z}$ is the correlation length of the ''space'' scale and the scaling function behaves as $f(y)\propto y^{H}$, if $y\ll 1$, or $f(y)\approx 1$, if $y\gg 1$; here H is the so-called local randomness (or Hurst) exponent; z is the dynamic exponent, and $\beta=H/z$ is the growth exponent [5]. The Hurst exponent [6] gives an indication of whether the system behavior is random ($H=0.5$) or displays persistence ($0.5<H<1$) or antipersistence ($0\leqslant H<0.5$) [4].

The scaling form (1) is valid for a large variety of systems far from equilibrium, as well as for critical phenomena [1]. Specifically, the Family-Viscek dynamic scaling ansatz is commonly applied to describe the kinetic roughening of growing interfaces [4]. However, generally, a simple scaling law (1) does not hold [2,3], instead there is an evidence that the logarithms of the parameters can be used to produce a data collapse [3]. In this way, Sittler and Hinrichsen [3] have suggested the general dynamic scaling form with continuously varying scaling exponents [7]

$$\sigma(\Delta,t)\propto\Phi(\Delta^{H(\Delta,t)},t^{\beta(\Delta,t)}), \tag{2}$$

where Φ is the scaling function. Examples of systems displaying the general scaling dynamics (2) include certain self-organized critical sand pile models [8], ion sputtering of surfaces [9], and DLA-related growth processes [10]. The continuously varied scaling exponents were found in some experiments in turbulence [11], in paper wetting experiments [12], in numerical analysis of Kuramoto-Sivashinsky equation [13], and also were observed in Monte Carlo simulations of ion etch-front roughening [14].

The dynamics of financial markets has recently becomes a focus of interest to physicists because of its rich and complex scaling behavior analogous to that commonly observed in physical systems with many interacting units [15]. Many statistical properties of financial markets have already been explored, and have revealed striking similarities between price volatility dynamics and the kinetic roughening of growing interfaces [16]. Accordingly, physical models have been shown to have wide application to understanding the dynamics of stock markets [17]. This allows us to use the dynamic scaling approach to study the kinetic roughening of growing interfaces [18], as well as the financial time series. In this way, we expect that the scaling analysis of economic time series might yield novel results, providing new insights into dynamics of very different complex systems [19]. In this work, the general dynamic scaling approach is used to study the scaling properties of crude oil market.

II. GENERALIZED SCALING DYNAMICS OF CRUDE OIL MARKET

The world oil is a capital-intensive environment characterized by complex interactions deriving from the wide variety of products, transportation-storage issues, and stringent environmental regulation. Crude oil is the world's most actively traded commodity, accounting for about 10% of total

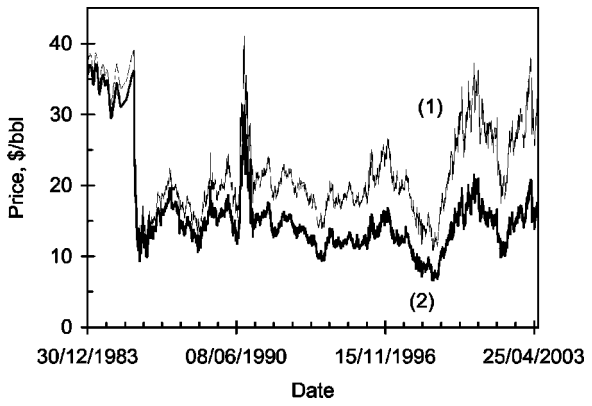

FIG. 1. Time records of West Texas Intermediate crude oil spot price in the current (1) and in the 1983 constant (2) dollars per barrel, $/bbl (source: Bloomberg database [25]). The graphs correspond to the period from 30 December 1983 to 23 June 2003.

world trade [20]. The crude oil market is characterized by extremely high levels of price volatility. Fluctuations in crude oil price are caused by supply and demand imbalances arising from events such as wars, changes in political regimes, economic crises, formation breakdown of trade agreements, unexpected weather patterns, etc. [21] At the same time, many of the price forecasting models are based on the belief that historical price series exhibit some statistical properties that permit to predict future price movements [22].

A. Data analyzed

To quantify the scaling dynamics of crude oil market, we studied the daily records of the spot prices [23] $P(t)$ [see Figs. 1 and 2(a)] and the price volatilities $V_n(t)$ [see Figs. 2(b)–2(d)] from the West Texas Intermediate [24] (WTI) crude oil price listings [25]. Specifically, we analyze the WTI

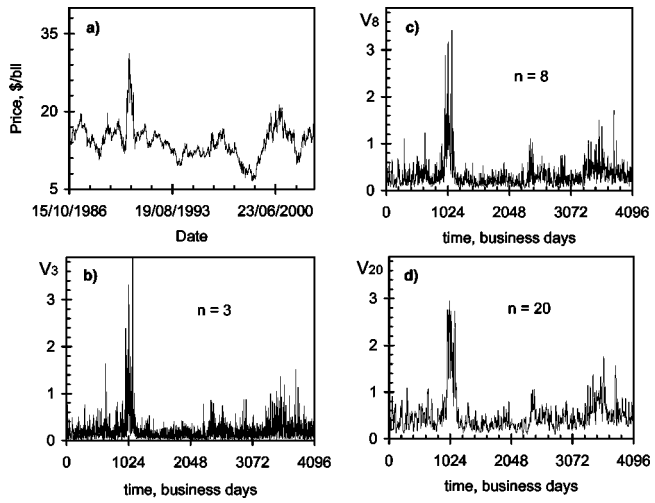

FIG. 2. (a) Time record of West Texas Intermediate crude oil spot price in the 1983 constant dollars per barrel ($/bbl); and (b)–(d) realized price volatilities for the period of 4096 business days for different horizons: (b) $n=3$, (c) $n=8$, and (d) $n=18$ business days. All time series correspond to the period from 15 October 1986 to 23 December 2002.

crude oil price in constant 1983 US dollars [26] over the period from 30 December 1984–23 June 2003 representing 5181 observations (weekends and business holidays are excluded). Then we construct 699 time series of realized volatility [27]

$$V_n(t)=[\langle P^2(t)\rangle_n-\langle P(t)\rangle_n^2]^{1/2} \tag{3}$$

of length $T=4096$ business days (about 16 business years), for different time horizons $n=2,3,...,700$ (from 2 business days to about 3 business years), where t is the business time and $\langle\cdots\rangle_n$ denotes the business time average within a window of size n. In this study, all records of volatility [see Figs. 2(b)–2(d)] correspond to the period from 15 October 1986 to 23 December 2002 [28]. One can see that the price volatility changes from day to day in such a way that time series of volatilities $V_n(t)$ realized at different time intervals n look similar.

B. Scaling analysis techniques

To detect and quantify the dynamic scaling behavior of price volatility within a framework of interface roughening dynamics, here the volatility horizon n is treated as an analog of time variable (t), while the business time t is treated as an analog of lateral extent (X) of growing interface. Accordingly, the price volatility fluctuations are characterized by the analog of interface height fluctuations [4], defined as

$$\sigma(n,\tau)=\langle[V_n(t)-\langle V_n(t)\rangle_\tau]^2\rangle_R^{1/2}\propto\Phi(\tau^{H_n},n^{\beta(\tau)}), \tag{4}$$

where $\langle\cdots\rangle_\tau$ denotes the business time average within a window of size τ and $\langle\cdots\rangle_R$ denotes the average over different realizations.

To characterize the scaling properties of time series, within a framework of the general dynamic scaling concept (2), (4) the volatility growth exponent $\beta(\tau)$ can be determined from the scaling behavior

$$\sigma(n,\Delta)\propto n^{\beta(\tau)} \tag{5}$$

for different intervals of business time τ. To test the correlations in business time scale ($\tau\leqslant T=4096$) we studied the autocorrelation functions [29]

$$C(\tau)=\langle P(t+\tau)P(t)\rangle_T/\langle P^2(t)\rangle_T$$

and

$$C_n(\tau)=\langle V_n(t+\tau)V_n(t)\rangle_T/\langle V_n^2(t)\rangle_T, \tag{6}$$

where the angle brackets denote the time average. The behaviors of correlation function at $\tau\to0$ and $\tau\to T\to\infty$ characterize the stochastic ''memory'' of the time series. Furthermore, the scaling behavior of the price volatility was also investigated by calculating the structure factor or power spectrum

$$S_n(\omega)=\langle\hat{V}_n(\omega)\hat{V}_n(-\omega)\rangle\propto\omega^{(2H_n+1)}F_n(\omega n^{1/z(n,\tau)}), \tag{7}$$

where $\hat{V}_n(\omega)=T^{-1/2}\int_T[V_n(t)-\langle V_n(t)\rangle_T]\exp(i\omega\tau)dt$ is the Fourier transform of the volatility record $(\cdots)$ and $F(y)$ is the scaling function, such that $F_n(y)\propto y^H$, if $y\ll 1$, or $F_n(y)\approx 1$, if $y\gg 1$. The precise form of the autocorrelation function is, however, not known. This makes difficult to use Eqs. (6), (7) for the quantitative measure of Hurst exponent for finite time series.

To quantify the intensity of long range correlations, the local randomness (Hurst) exponents of $P(t)$, as well as of each time record $V_n(t)$, were determined by five methods adopted from the BENOIT 1.3 software [30]: the rescaled-range analysis, the roughness length, the variogramm, the power-spectrum, and the wavelet methods. The rescaled-range analysis is one of the oldest and best-known methods for determining H. This method was proposed by Mandelbrot and Wallis [31] and is based on previous hydrological studies of Hurst [32]. The rescaled range R/σ is defined as the ratio of the maximal range of the integrated signal (R) normalized to the standard deviation (4). For time series characterized by long-range correlations the expected value of rescaled range scales as $R/\sigma\propto\tau^H$. If the time record possesses only short-range correlations then the log-log plot of R/σ is also a straight line with slope 0.5. Lo [33], however, showed that this method may be significantly biased when there is short-term dependence in the form of heteroskedasticity or autocorrelation. The roughness-length and variogramm methods are based on the scaling behavior of the standard deviation $\sigma_n\propto(\tau)^{H_n}$ and the semivariance Var $\propto\tau^{2H}$. Problems with these methods are that the choice of the sampling interval, as well as the determination of the slope of the plot, may affect the result of Hurst exponent estimation. Power spectral methods are based on power spectral analysis, which can be applied to time series data. The power spectral density function (7) for random data describes the data in terms of spectral density of its mean square value for different frequencies and scales as $S_n\propto\tau^{-2H_n-1}$. The Fourier transform uses cosines, sins and exponentials to represent a time record, and so it is more useful for representing linear functions and it is less suitable for analyzing nonlinear chaotic time series. Wavelets offer an alternative method to analyze complex time series [34]. The Wavelet method is based on the property that Wavelet transforms of the self-affine traces have self-affine properties. This method is appropriate for analysis of nonstationary series, i.e., where the variance does not remain constant with increasing length of the data set. Wavelets are similar to, but an extension of Fourier analysis and the wavelet transform is computationally similar in principle to the fast Fourier transform. The aim of the wavelet transform is to express an input signal into a series of coefficients of specified ''energy.'' The discrete numbers associated with each coefficient contain all the information needed to completely describe the series provided one knows which analyzing wavelet was used for the decomposition. Wavelet transforms makes use of scaling functions that have the property of being localized in both time and frequency. A scaling coefficient $w\propto a^{H_n+1/2}$ characterizes and measures the width of a wavelet, where a denotes a scale parameter [35]. The statistical distributions of crude oil price and realized price volatilities were analyzed with the help of @RISK software [36], which ranks the fitted distributions using three test statistics: χ^2, Anderson-Darling, and Kolmogorov-Smirnov statistics [37].

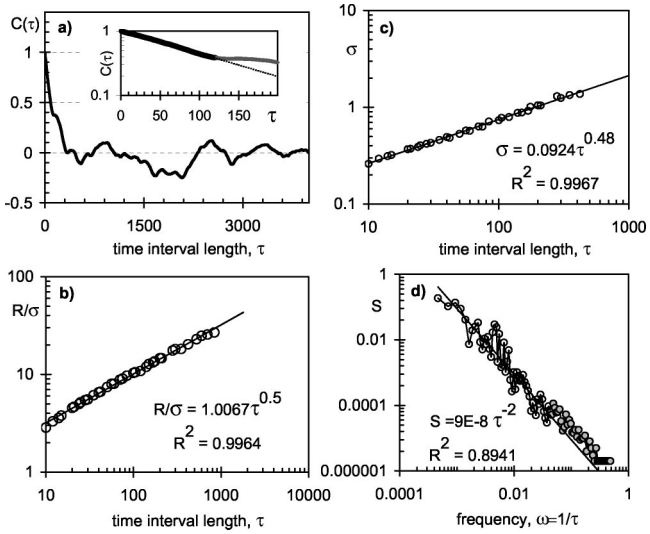

FIG. 3. (a) Autocorrelation function of price record shown in Fig. 2(a) [the inset shows $C(\tau)$ in semilog coordinates] and (b)–(d) fractal graphs of price record obtained by (b) the rescaled range, (c) the roughness length, and (d) the power spectrum methods (time interval length in business days).

C. Results and discussion

We find that the autocorrelation function [Fig. 3(a)] of crude oil price record [Fig. 2(a)] decays exponentially [see inset in Fig. 3(a)] as $C\propto\exp(\tau/\tau_0)$, with a characteristic time $\tau_0=120$ business days (about the half business year). Furthermore, we find that the Hurst exponent of price record is equal to $H=0.50\pm0.02$ [see Figs. 3(b)–3(d) and 4] [38]. This means that there are no long-range correlations in the crude oil price record. This is consistent with the finding that the crude oil spot price distribution is a symmetric logistic distribution [see Fig. 5(a)], which provides the best fitting of data according to three test statistics mentioned above.

At the same time, we find that the realized volatilities [Fig. 2(b)–2(d)] possess a statistical self-affine invariance

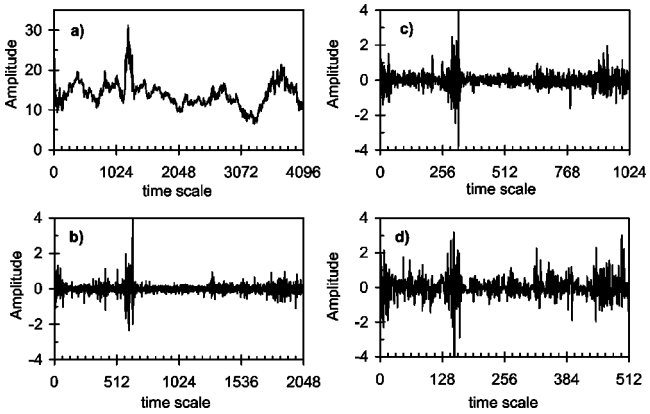

FIG. 4. (a) Price record as in Fig. 2(a) and (b)–(d) three first wavelets (time scale in business days, $H_W=0.50$).

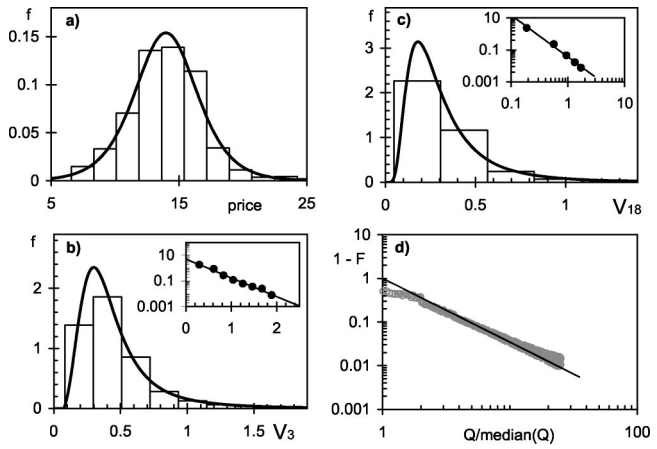

FIG. 5. (a) Conditional probability distribution of crude oil price in \$/bbl (bins: experimental data, solid lines: fitting by the logistic distribution). (b) Conditional probability distributions of price volatility for horizon $n=3$ [bins: experimental data, solid lines fitting by the Pearson distribution (15) (p value is 0.41), inset: the distribution tail in the semilog coordinates]. (c) Conditional probability distributions of price volatility for horizon $n=18$ [bins: experimental data, solid lines: fitting by the log-logistic distribution (17) (p value is 0.38), inset: the distribution tail in the log-log coordinates]. (d) Cumulative distribution of normalized avalanches in log-log coordinates [circles: experimental data, solid lines: the graph of Eq. (19); the squared coefficient of correlation between the data and theoretical line is equal to $R^2=0.9549$].

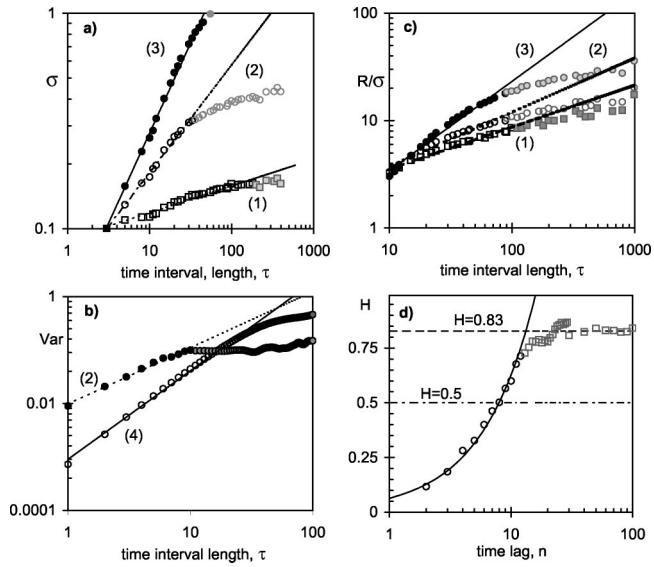

FIG. 6. (a)–(c) Fractal graphs of price volatility records shown in Figs. 2(b)–2(c) obtained by (a) the roughness length, (b) the variogram, and (c) the rescaled-range methods [numbers correspond to different horizons: (1) corresponds to $n=3$, (2) corresponds to $n=8$, (3) corresponds to $n=20$, and (4) corresponds to $n=60$ business days]. (d) Horizon dependence of the Hurst exponent (values of H_n are averaged through five methods) in the semilog coordinates [time scale in business days, circles and squares: experimental data, solid line: data fitting by Eq. (8), $R^2=0.9882$].

within wide ranges of business time scale $[3<\tau<\tau_C(n)]$ characterized by well defined Hurst exponent H_n for each horizon n [39] [see Figs. 6(a)–6(d)]:

$$H_n=0.0621n, \quad \text{when } n\leqslant 12 \tag{8}$$

and

$$H_n=0.83\pm 0.04, \quad \text{when } n\geqslant 18. \tag{9}$$

Our finding means that the long horizon realized volatilities ($n>8$) are persistent, i.e., volatility increments are positively correlated in business time, whereas the short-horizon volatilities ($n<8$) are antipersistent, i.e., $V_{n<8}(t)$ displays negative autocorrelations in business time.

Furthermore, we find that the transition from antipersistent to persistent volatility at $n=8$ is accompanied by an abrupt change in the behavior of $\min_n\{V_n(T=4096)\}$ versus n [Fig. 7(a)], nevertheless the time-average and the standard deviations of $V_n(\tau)$ have no anomaly at $n=8$ [see Fig. 7(b)]. Specifically, the time averaged volatility behaves as $\langle V_n(\tau)\rangle_{\tau=4096}\propto n^{0.5}$ up to $n=700$, while the standard deviation of realized volatility behaves as $\sigma(\tau=T=4096)\propto n^{0.25}$ up to $n=18$, but it scales as $\sigma\propto n^{0.5}$, when the realized volatility is characterized by the constant Hurst exponent $H=0.83\pm 0.04$.

Moreover, we find that the growth exponent behaves as [see Figs. 7(b), 7(c)]

$$\beta=0.25\tau_C/\tau \text{ if } \tau<\tau_C(n) \text{ and } \beta=0.25 \text{ if } \tau>\tau_C(n), \quad \text{when } n<18, \tag{10}$$

$$\text{while } \beta=0.5 \text{ for any } \tau, \text{ when } n>18. \tag{11}$$

We also find that the interval of correlations τ_C in the business time scale increases with the horizon of volatility as $\tau_C\propto n^{z(n,\tau)}$, where the dynamic exponent is a function of n and τ if $n<18$, while $z=H/\beta=1.66$ for long horizons $n>18$ [see Fig. 7(d)].

Accordingly, we find that the long-horizon volatility ($n\geqslant 18$) satisfies the Family-Viscek dynamic scaling ansatz (1), whereas for horizons smaller than 18 business days the crude oil price volatility satisfies the generalized dynamic scaling law [3]

$$\sigma(n,\tau)\propto F^{\cdot\cdot}((\tau)^{H(n)},n^{\beta(\tau)}), \tag{12}$$

with continuously varying scaling exponents (8) and (10), which are quasihomogeneous functions satisfying the partial differential equation [7]

$$\frac{\partial\ln(H_n)}{\partial\ln(n)}=-\frac{\partial\ln(\beta)}{\partial\ln(\tau)}=1. \tag{13}$$

This implies that scaling function F possesses a local scaling invariance [3], i.e.,

$$F((\lambda\tau)^{H(n)},(\lambda n)^{\beta(\tau)})=\lambda F^{\cdot\cdot}((\tau)^{H(n)},n^{\beta(\tau)}), \tag{14}$$

where λ is a dilatation parameter and $n<18$, $\tau<\tau_C$.

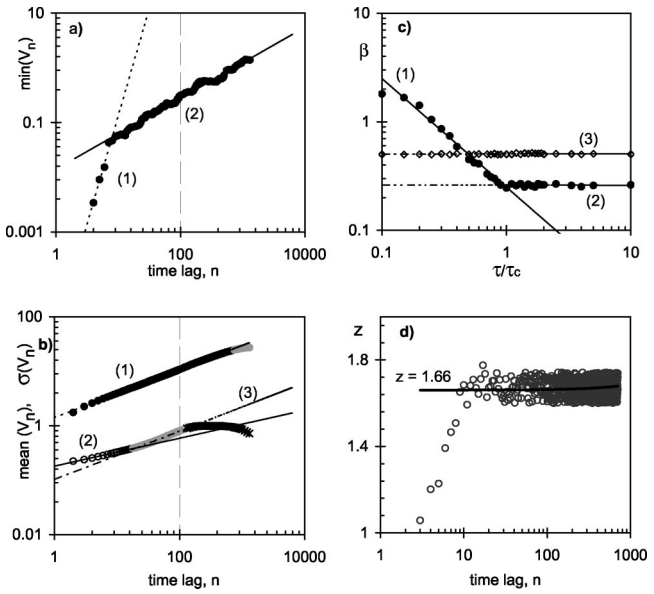

FIG. 7. Results of the scaling analysis of crude oil price volatility. (a) The minimum of realized volatility versus time horizon [points: experimental data, lines: power law fits (1) $\min(V_n)=10^{-5}n^{3.95}$, $R^2=0.97$ and (2) $\min(V_n)=0.014n^{0.66}$, $R^2=0.993$]. (b) The mean (1) and the standard deviation (2,3) of realized volatility ($\tau=4096$) versus time lag, n [points: experimental data, lines: power law fittings. (1) $\langle V_n(\tau=4096)\rangle_\tau=1.5n^{0.5}$, $R^2=0.999$, (2) $\sigma\{V_n(\tau=4096)\}=0.18n^{0.26}$, $R^2=0.995$, and (3) $\sigma\{V_n(\tau=4096)\}=0.1n^{0.45}$, $R^2=0.998$; the y axis labels indicate the quantity]. (c) The volatility growth exponent β versus normalized time interval for volatility horizons $n=3$ (1,2) and $n=60$ (3); points: results of analysis, lines: fitting by Eqs. (10) and (11). (d) Horizon dependence of dynamic exponent for price volatility (time scale in business days).

The crossover from antipersistent to persistent behavior indicates the existence of intrinsic horizon scale of price volatility (see Ref. [40]), $n_C\approx 8$. To get a deeper insight into the price volatility dynamics, we also perform the statistical analysis of volatilities $V_n(\tau)$ and avalanches defined as $Q(n,\tau)=V_{n+1}(\tau)-V_n(\tau)$.

We find that for short time horizons $n\leqslant 8$, the conditional probability of realized volatility is best fitted by the light-tailed Pearson distribution [Fig. 5(b)]

$$f(V_n)=\frac{(V_n-\phi)^{-(\gamma+1)}}{\rho^{-\gamma}\Gamma(\gamma)}\exp\left(\frac{V_n-\phi}{\rho}\right) \tag{15}$$

with horizon dependent parameters

$$\rho=0.48n^{034}(R^2=0.95) \quad \text{and} \quad \phi=0.13n^{-0.69}(R^2=0.97) \tag{16}$$

and $\gamma=3.6\pm 01$; $\Gamma(\gamma)$ is the gamma function.

At the same time, for the larger time horizons, $n>8$, the conditional probability of realized volatility is the log-logistic distribution [Fig. 5(c)]:

$$f(V_n)=\frac{\gamma[(V_n-\phi)/\rho]^{\gamma-1}}{\rho\{1+[(V_n-\phi)/\rho]^{\gamma}\}^2}, \tag{17}$$

where $\gamma=2.55\pm 0.07$ [41] and

$$\rho=0.104n^{0.385}(R^2=0.998), \quad \phi=0.0082n^{0.744}(R^2=0.996); \tag{18}$$

i.e., the long-horizon volatility distribution is fat tailed, but it is well outside the stable Lévy range $0<\gamma<2$ [42].

Furthermore, we find that the statistical distribution of avalanches is also best fitted by the log-logistic distribution with $\phi=0$, $\rho=0.75n^{-0.68}$ and $\gamma=1.46\pm 0.02$ (the p value is 0.48); obeying a power law tail [see Fig. 5(d)]:

$$F\propto 1-\{Q/\text{median}[Q(\tau)]\}^{-1.46} \tag{19}$$

with the scaling exponent γ within the stable Lévy range [41].

This indicates that observed behavior of crude oil price volatility can be interpreted in terms of scale-free avalanches, which define the intrinsic horizon scale and build up long-range correlations in the price volatility [43]. Such a behavior can be modeled with the use of Kuramoto-Sivashinsky equation [13] with white or correlated noise.

III. CONCLUSIONS

We show that the time series of price volatility can be analyzed within a framework of kinetic roughening of moving interface, treating the length of series as an analog of spatial variable and the horizon of volatility as an analog of time variable. In this way we find that crude oil volatility possesses a general dynamic scaling behavior. Furthermore, we observe a transition from antipersistent to persistent behavior of the volatility in the horizon scale. This transition is accompanied by the change in the type of volatility distribution, which is light-tailed for short horizons and it is heavy-tailed for long horizons.

Our findings have potentially wide-ranging implications in econophysics [44], as well as in statistical physics of complex systems. Specifically, we expect that the crossover from antipersistent to persistent behavior should be observed in a wide variety of systems displaying generalized scaling dynamics with continuously varying exponents [45]. The existence of a ''universal'' mechanism which gives rise to crossover from antipersistent to persistent behavior in systems of different nature could provide a new insight to the physics of complex systems governed by avalanche dynamics leading to generalized scaling dynamics with continuously varying exponents.

ACKNOWLEDGMENTS

The authors would like to thank J. M. Lopez for useful discussions. This work has been supported by the CONACYT of the Mexican Government (Project No. 3495-U).

[1] P. Bak, *How Nature Works: The Science of Self-Organized Criticality* (Copernicus, New York, 1996).

[2] J. J. Ramasco, J. M. López, and M. A. Rodríguez, Phys. Rev. Lett. **84**, 2199 (2000).

[3] L. Sittler and H. Hinrichsen, J. Phys. A **35**, 10 531 (2002).

[4] A.-L. Barabási and H. E. Stanley, *Fractal Concepts in Surface Growth* (Cambridge University Press, Cambridge, 1995).

[5] In the absence of any characteristic scale the fluctuations are expected to be self-affine. However, commonly the dynamic scaling is characterized by three or more independent scaling exponents. Specifically, according to the concept of generic dynamic scaling [4], the interface roughening dynamics is characterized by six scaling exponents, four of which may be independent.

[6] The Hurst exponent is related to the fractal dimension of graph $Z(X)$ as $D_F=d-H$, where d is the topological dimension of embedded space [4].

[7] It should be pointed out that the functional form of scaling exponents cannot be chosen freely; rather their functional dependence is constrained by a group homomorphism linking the concepts of generalized and ordinary scaling [3].

[8] C. Tebaldi, M. De Menech, and A. L. Stella, Phys. Rev. Lett. **83**, 3952 (1999).

[9] J. T. Drotar, Y.-P. Zhao, T. M. Lu, and G.-C. Wang, Phys. Rev. E **59**, 177 (1999).

[10] B. Hinnemann, H. Hinrichsen, and D. Wolf, Phys. Rev. Lett. **87**, 135701–135704 (2001).

[11] X.-Z. Wu, L. Kadanoff, A. Libchaber, and M. Sano, Phys. Rev. Lett. **64**, 2140 (1999).

[12] A. S. Balankin and D. Morales Matamoros, in *Emergent Nature*, 1st ed., edited by M. M. Novak (World Scientific, London, 2001), Vol. 1, pp. 345–356.

[13] J. Buceta, J. M. Pastor, M. A. Rubio, and F. J. Rubia, Physica D **113**, 166 (1988).

[14] J. T. Drotar, Y.-P. Zhao, M.-T. Lu, and G.-C. Wang, Phys. Rev. B **61**, 3012 (2000).

[15] R. N. Mantegna and H. E. Stanley, Nature (London) **376**, 45 (1995); J. P. Sethna, K. A. Dahmen, and Ch. R. Myers, *ibid.* **410**, 242 (2001); Y. Lee, L. A. Nunes Amaral, D. Canning, M. Meyer, and H. E. Stanley, Phys. Rev. Lett. **81**, 3275 (1998); V. Plerou, P. Gopikrishnan, B. Rosenow, L. A. Nunes Amaral, and H. E. Stanley, *ibid.* **83**, 1471 (1999); R. Friedrich, J. Peinke, and Ch. Renner, *ibid.* **84**, 5224 (2000); V. Plerou, P. Gopikrishnan, and H. E. Stanley, Nature (London) **421**, 130 (2003).

[16] Y. Liu, P. Gopikrishnan, P. Cizeau, M. Meyer, Ch.-K. Peng, and H. E. Stanley, Phys. Rev. E **60**, 1390 (1999); V. Plerou, P. Gopikrishnan, L. A. Nunes Amaral, M. Meyer, and H. E. Stanley, *ibid.* **60**, 6519 (1999); P. Gopikrishnan, V. Plerou, L. A. Nunes Amaral, M. Meyer, and H. E. Stanley, *ibid.* **60**, 5305 (1999); V. Plerou, P. Gopikrishnan, L. A. N. Amaral, X. Gabaix, and H. E. Stanley, *ibid.* **62**, R3023 (2000); V. Plerou, P. Gopikrishnan, X. Gabaix, and H. E. Stanley, *ibid.* **66**, 027104 (2002); K. Matia, L. A. N. Amaral, S. P. Goodwin, and H. E. Stanley, *ibid.* **66**, 045103 (2002); X. Gabalx, P. Gopikrishnan, P. Plerou, and H. E. Stanley, Nature (London) **423**, 267 (2003).

[17] B. B. Mandelbrot, *Fractals and Scaling in Finance* (Springer, New York, 1997); J. P. Bouchaud and M. Potters, *Theory of Financial Risk: From Statistical Physics to Risk Management* (Cambridge University Press, Cambridge, 2000).

[18] A. S. Balankin, O. Susarrey, and J. Marquez Gonzales, Phys. Rev. Lett. **90**, 096101 (2003); A. S. Balankin, D. Morales, and I. Campos, Philos. Mag. Lett. **80**, 165 (2000); A. S. Balankin, A. Bravo Ortega, and D. Morales Matamoros, *ibid.* **80**, 503 (2000); A. S. Balankin and D. Morales Matamoros, *ibid.* **81**, 495 (2001).

[19] There is a huge amount of high frequency economic data available, which can be treated with methods developed in physics of complex systems.

[20] S. Galina-Hidalgo, D. Romo, and A. Pérez, J. Energy Development **28**, 57–68 (2002).

[21] M. C. Lynch, J. Energy Development **28**, 107 (2002).

[22] T. J. Considine and H. Eunnyeong, Energy Economics **22**, 527 (2000).

[23] In the cash market, purchases and sales of the commodity for immediate delivery occur at a price that is referred as the ''spot price,'' in contrast to the forward and future prices, associated with forward and future contracts, respectively.

[24] Crude oil prices are slightly different worldwide, however between prices markers (Brent, Dubai, and West Texas Intermediate) are not large and they correlate closely which each other [22,25].

[25] URL: http://www.bloomberg.com

[26] Crude oil has been traded on the New York Mercantile Exchange (NYMEX) since 1983.

[27] Although it is common to talk about the price volatility, there is no single universally accepted definition of this parameter. Various measures of price volatility can be constructed, in particular the absolute values of price (or logarithms of price) returns, the standard deviation of price returns, etc. [5–7]. In finance, it is typically characterized in terms of the standard deviation of prices at a particular time scale [see, for example, G. Bomer, Active Trader **2**, 86 (2003)].

[28] We also studied records corresponding to the period from 09 April 1987 to 23 June 2003.

[29] K. Falconer, *Techniques in Fractal Geometry* (Wiley, New York, 1997).

[30] W. Seffens, Science **285**, 1228 (2000).

[31] B. B. Mandelbrot and J. R. Wallis, Water Resour. Res. **4**, 909 (1969).

[32] H. E. Hurst, Trans. Am. Soc. Civ. Eng. **116**, 770 (1951).

[33] A. W. Lo, Econometrica **59**, 1279 (1991).

[34] Z. R. Struzik, Physica A **296**, 307 (2001).

[35] The mother wavelet in BENOIT 1.3 software is a step function.

[36] @RISK 4.5, URL http://palisade.com

[37] W. J. Conover, *Practical Nonparametric Statistics*, 2nd ed. (Wiley, New York, 1980).

[38] This value was determined by five methods mentioned above and it is not sensitive to the sampling period. Moreover, we also determine the global scaling exponent α (see Ref. [2]) from the scaling behavior $R=\langle \max_{t\in T} P(t)-\min_{t\in T} P(t)\rangle_R \propto T^{\alpha}$ and find that $\alpha=H=0.50\pm 0.03$.

[39] Different methods lead to slightly different values of H_n; for example, for $n=8$ we obtain $H_{R/\sigma}=0.467$, $H_{\sigma}=0.508$, $H_{Var}=0.492$, $H_S=0.477$, and $H_W=0.565$, and so $H_8=0.50\pm 0.04$ [see also Figs. 3(b)–3(d), 4, and 6(a)–6(c)].

[40] Wen-Tau Juan and I. Lin, Phys. Rev. Lett. **80**, 3073 (1998).

[41] We find that γ is independent of the horizon of volatility for time lags $n>8$.

[42] It should be pointed out that the parameters of volatility distributions, as well as the scaling exponents in Eqs. (1) and (14), are not sensitive to the sampling period. Essentially the same results were also obtained for the period from 9 April 1987 to 23 June 2003.

[43] Our findings suggest that the dynamics of price volatility is governed by self-organized criticality (SOC), similar to that which is commonly illustrated conceptually with avalanches in a pile of sand grains. The most essential feature of the SOC is that the system jumps from one metastable state to another by avalanche dynamics up to critical state without external forcing. Accordingly, the price volatility evolves through transient states at time horizons $n<18$, which are not critical, to a dynamical attractor poised at criticality for long-time horizons, when volatility obeys the Family-Viscek dynamic scaling (1) and could therefore be predictable in statistical sense.

[44] Accurate modeling and forecasting of commodity price volatility is of paramount importance in risk management and option pricing.

[45] We note that Monte Carlo simulations of reactive ion etch-front roughening [9] described by the Kuramoto-Sivashinsky equation predict the generalized scaling dynamics with time-dependent roughness exponent and continuous transition from antipersistent to persistent front roughness regime. This allows a possibility to use a similar model for simulations of realized and employed volatility of crude oil prices. Unfortunately, the crossover from antipersistent to persistent roughness was not discussed in Ref. [9].